Available online at www.sciencedirect.com

ScienceDirect

IFAC Papers Online CONFERENCE PAPER ARCHIVE

IFAC-PapersOnLine 48-9 (2015) 150–155

Modeling and Control of the tPVTOL ⋆

J.G.Villagómez, M.Vargas, M.G.Ortega, F.R.Rubio

Dpt. Systems Engineering and Automation. Univ. of Seville, Spain

{villagomez,vargas,mortega,rubio}@us.es

Abstract: This paper presents the modeling and control of a planar multibody aerial platform, composed of a Miniature Vertical Take-Off and Landing Aerial Platform (MAV-VTOL) and a camera positioning system. The goal is to improve the current operational profile of visual sensors onboard the MAV, by broadening current aerial configurations for visual sensors tasks with novel capabilities to disengage the dynamic coupling due to typical setups. The Newton-Euler and Euler-Lagrange formalisms are simultaneously applied aiming at obtain and verify coupling terms between the aerial and the camera positioning system. Results of linear and nonlinear control techniques applied to control the position and orientation of the camera frame onboard the MAV are presented.

Keywords: Multi-body mechanics, Fly-the-camera, Multi-rotor nonlinear control, Aerial manipulation.

1. INTRODUCTION

The development and application of Miniature Air Vehicles (MAV) provides an excellent alternative to typical aerial platforms due to its operational functionalities, such as vertical take-off and landing (VTOL) or maneuverability and hovering, to name a few. The range of electromechanical devices to be attached to the frame, in order to enhance its current functional profile is quite constrained, mainly due to the payload inherent limitations. Works where the modeling of a system compounded by an industrial manipulator and an aerial platform have been recently presented (Kondak et al. (2014)). Whereas this concept is quite promising, with applications such as aerial grasping or cargo transportation, represents new challenges in control theory (Kim et al. (2013)).

It is possible to consider other MAV applications, where it would be necessary, e.g., the use of an actuated optical sensor onboard the MAV (Altug et al. (2002)). By combining the 3 translational DOF plus the yaw angle provided by the motion of a MAV with the 2 rotational DOF supplied by a camera positioner, or camera *gimbal*, it is possible to position the six degrees of freedom of the onboard camera. Previous works already considered this alternative, known as "fly-the-camera", but only to improve the camera operator experience (Neff et al. (2007)). In contrast, what we propose is the full automation of the compounded system. As a first approach to the task of modeling and control, the model under consideration is a planar assumption of the full roll-tilt VTOL multi-body system, hereby stated as tilt-PVTOL. All references will be given in the camera frame (Villagomez et al. (2014a)), and corresponding dynamic model is hereby obtained. Other considerations are also valid, such as considering the camera evolving and references given in the MAV frame (Villagomez et al. (2014b)).

The outline of this work is organized as follows: section II describes the procedure followed to compute the dynamic model of a camera moving in the space through the constrained motion in a plane of a MAV with a camera positioner. Linear and nonlinear control techniques are respectively proposed to stabilize the flight of the camera in sections III and IV. Numerical results are presented in Section V to validate the design of the nonlinear controllers, and final remarks and perspectives are given in section VI.

2. SYSTEM MODELING

For modeling the mechanics of the system under consideration we introduce a variation of the well-known Planar Vertical Take-Off and Landing (PVTOL) aircraft problem (Castillo et al. (2005)), with the addition of a camera positioner in configuration $roll-tilt$, in the vertical plane. This model will be called tPVTOL (*tilt* PVTOL). Consider a 1 DOF camera positioner system evolving within the plane, thanks to the flight of a miniature rotorcraft, which it is rigidly mounted to. The camera actuator is intended to keep a desired camera inertial orientation, during near-hovering or in-motion maneuvers rejecting disturbances. The in-flight camera positioning operation shifts the rotorcraft center of gravity (CoG), generating reaction forces and consequently disturbing the inertial camera orientation (Orsag et al. (2013)).

2.1 Reference Frames and Notation

The kinematics of the flying system comprises three right-handed reference coordinate frames. Let $(\hat{\boldsymbol{x}}_{\mathcal{W}}, 0, \hat{\boldsymbol{z}}_{\mathcal{W}})$, which defines the fixed inertial frame $\mathcal{W}$, for the planar case, whose origin $\mathcal{O}_{\mathcal{W}}$ is located at the Earth surface. Let: $(\hat{\boldsymbol{x}}_{\mathcal{B}}, 0, \hat{\boldsymbol{z}}_{\mathcal{B}})$ be the body-fixed frame $\mathcal{B}$ for the planar case, whose origin $\mathcal{O}_{\mathcal{B}}$ represents the MAV's center of masses

⋆ This work was partially supported by the spanish Ministry of Education (MECD) under national research projects $DPI2012-37580-C02-02$ and $DPI2013-44135-R$.

Peer review under responsibility of International Federation of Automatic Control.
10.1016/j.ifacol.2015.08.075

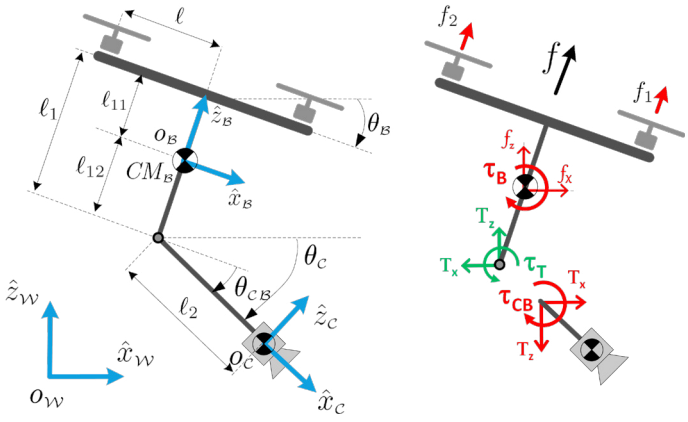

Figure 1. Freebody diagram: (a) tPVTOL Frames of reference and (b) depiction (in red) of applied forces and moments.

($CM_{\mathcal{B}}$) location. The camera fixed frame $\mathcal{C}$ can be denoted as $(\hat{\boldsymbol{x}}_c, 0, \hat{\boldsymbol{z}}_c)$, whose origin $\mathcal{O}_c$ corresponds to the center of the camera frame. The orientation of the rigid body is given by a rotation $\mathbf{R}: \mathcal{B} \to \mathcal{W}$, with $\mathbf{R} \in SO(2)$. $\theta_{\mathcal{B}}$ is denoted as the MAV's inertial pitch angle; θ_c as the inertial angle of the camera positioner (the camera's *tilt* inertial angle) and $\theta_{c\mathcal{B}}$ is the angular difference between the MAV's *pitch* angle and the camera's inertial frame *tilt* angle. Links ℓ_{11}, ℓ_{12} and ℓ_2 represents system lengths, as depicted in (Fig. 1).

Conceptually four control signals are designed to control the rotational ($[\tau_{\mathcal{B}}\ \tau_{c\mathcal{B}}]$) and translational ($[f_x\ f_z]$) subsystems: the control input $\mathbf{f} = [f_x\ f_z]^\top = \mathbf{R}(\theta_{\mathcal{B}}) \cdot [0\ f]^\top$ as the thrust vector, where $f = f_1 + f_2$ is the total upward thrust in the body frame, which generates a reaction torque defined as $\tau_{\mathcal{B}} = (f_2 - f_1)\ell$; and the camera positioner rotational joint torque, labelled as $\tau_{c\mathcal{B}}$. ℓ is considered as the length between the position of each propeller and the geometric center of the airframe (symmetric frame). The instantaneous camera inertial position, defined as $\boldsymbol{\xi} = [x_c, z_c]^\top$ is achieved through the MAV heading's angle and the total upward thrust, while the camera's tilt angle is controlled by mixing control signal inputs $\tau_{\mathcal{B}}$ and $\tau_{c\mathcal{B}}$.

2.2 Newton-Euler Formalism

The equations of motion are first computed through the Newton-Euler formulation. The composite system can be first seen as two different bodies subject to external forces, applied to the center of mass of the MAV and the camera frame respectively, expressed in the body-fixed frame. Couplings are obtained according to Newton's third law. Similarly, forces applied in the MAV frame will be directly passed through the kinematic chain till the camera frame. Consequently, Newton's equations of motion yield the following dynamic model for que quad-rotor airframe:

$$\begin{cases} m_{\mathcal{B}}\ddot{x}_{\mathcal{B}} = f_x - T_x \\ m_{\mathcal{B}}\ddot{z}_{\mathcal{B}} = f_z + T_z - m_{\mathcal{B}}\mathrm{g} \\ I_{CM_{\mathcal{B}}}\dot{\omega}_{\mathcal{B}} = \tau_{\mathcal{B}} - \tau_T + T_x\ell_{12}\cos(\theta_{\mathcal{B}}) + T_z\ell_{12}\sin(\theta_{\mathcal{B}}) \end{cases} \tag{1}$$

The projection of the total upward thrust force is stated through components f_x and f_z. $\tau_{c\mathcal{B}}$ is the applied torque provided by the camera positioner rotational joint, generating reaction forces T_x and T_z and a reaction torque labelled as τ_T in the MAV frame. Excluding the total mass of the assembly comprising the camera and the positioner (henceforth Camera Composite System - CCS), the total mass of the quad-rotor is denoted as $m_{\mathcal{B}}$ with $I_{CM_{\mathcal{B}}}$ as the inertia mass-moment. $\dot{\omega}_{\mathcal{B}}$ is considered as the angular acceleration of the aircraft expressed in the inertial frame, and g is the gravitational constant. Since the dynamic model is computed from the camera frame perspective, the relationship is stated through the following coordinates

$$\begin{aligned} x_{\mathcal{B}} &= x_c + \ell_{12}\sin(\theta_{\mathcal{B}}) - \ell_2\cos(\theta_{c\mathcal{B}} + \theta_{\mathcal{B}}) \\ z_{\mathcal{B}} &= z_c + \ell_{12}\cos(\theta_{\mathcal{B}}) + \ell_2\sin(\theta_{c\mathcal{B}} + \theta_{\mathcal{B}}) \end{aligned} \tag{2}$$

Similarly, the dynamic model of the CCS is stated as follows:

$$\begin{cases} m_c\ddot{x}_c = T_x \\ m_c\ddot{z}_c = -T_z - m_c\mathrm{g} \\ I_c\dot{\omega}_{c\mathcal{B}} = \tau_{c\mathcal{B}} + T_x\sin(\theta_c)\ell_2 - T_z\cos(\theta_c)\ell_2 \end{cases} \tag{3}$$

with $\tau_T = \tau_{c\mathcal{B}}$, where I_c is the inertia mass-moment of the kinetic chain compounded by link ℓ_2 and camera, with total mass m_c, and $\dot{\omega}_{c\mathcal{B}}$ is the angular acceleration exerted by the camera frame expressed in the inertial frame.

2.3 Euler-Lagrange Formalism

In order to validate the model obtained through the Newton-Euler formalism, the study of the dynamic model by the decomposition of the resulting mechanical energy is proposed.

(1) Kinetic Energy
The total kinetic energy function $\mathcal{K}$ of the compounded mechanical system resulting from the translational and rotational motion can be partitioned by the sum of the MAV's kinetic energy, given by

$$\mathcal{K}_{\mathcal{B}} = \tfrac{1}{2}\, m_{\mathcal{B}}\, \left(\dot{x}_B^2 + \dot{z}_B^2\right) + \tfrac{1}{2}\, I_{CM_{\mathcal{B}}}\, \dot{\theta}_{\mathcal{B}}^2 \tag{4}$$

and the camera actuator's kinetic energy,

$$\mathcal{K}_c = \tfrac{1}{2}\, m_c\, (\dot{x}_c^2 + \dot{z}_c^2) + \tfrac{1}{2}\, I_c\, (\dot{\theta_{c\mathcal{B}}} + \dot{\theta}_{\mathcal{B}})^2 \tag{5}$$

where the position of the camera frame center is computed through:

$$\begin{aligned} x_c &= x_{\mathcal{B}} + \ell_2\, \cos(\theta_{\mathcal{B}} + \theta_{c\mathcal{B}}) - \ell_{12}\, \sin(\theta_{\mathcal{B}}) \\ z_c &= z_{\mathcal{B}} - \ell_2\, \sin(\theta_{\mathcal{B}} + \theta_{c\mathcal{B}}) - \ell_{12}\, \cos(\theta_{\mathcal{B}}) \end{aligned}$$

(2) Potential Energy
Considering $z_{\mathcal{B}}$ the height of the quad-rotor's CoG, the potential energy term $\mathcal{U}$ is given by the sum of both aircraft's and CCS's potential energies:

$$\mathcal{U} = \mathcal{U}_{\mathcal{B}} + \mathcal{U}_c = \mathrm{g}\, (m_{\mathcal{B}} z_{\mathcal{B}} + m_c z_c) \tag{6}$$

Once the kinetic and potential energy of the compounded system have been computed using (4), (5), and (6), and by definition:

$$\mathcal{L} = (\mathcal{K}_{\mathcal{B}} + \mathcal{K}_c) - (\mathcal{U}_{\mathcal{B}} + \mathcal{U}_c) \tag{7}$$

the Lagrangian $\mathcal{L}(\mathbf{q}_{\mathcal{L}}, \dot{\mathbf{q}}_{\mathcal{L}})$, denoted as $\mathcal{L}_{\mathcal{L}}$, can be written as follows:

$$\begin{aligned} \mathcal{L}_{\mathcal{L}} = {} & \tfrac{1}{2}\left(m\dot{x}_{\mathcal{B}}^2 + I_{CM_{\mathcal{B}}}\dot{\theta}_{\mathcal{B}}^2 + m_{\mathcal{B}}\dot{z}_{\mathcal{B}}^2 + m_c\dot{z}_{\mathcal{B}}^2 + \ell_{12}^2 m_c\dot{\theta}_{\mathcal{B}}^2\right) \\ & + m_c\dot{x}_{\mathcal{B}}\left(-\ell_2\left(\dot{\theta}_{\mathcal{B}}\mathrm{s}\left(\theta_{\mathcal{B}} + \theta_{c\mathcal{B}}\right) + \dot{\theta}_{c\mathcal{B}}\mathrm{s}\left(\theta_{\mathcal{B}} + \theta_{c\mathcal{B}}\right)\right) - \ell_{12}\dot{\theta}_{\mathcal{B}}\mathrm{c}\theta_{\mathcal{B}}\right) \\ & - \ell_2 m_c\left(\dot{\theta}_{\mathcal{B}}\dot{z}_{\mathcal{B}}\mathrm{c}\left(\theta_{\mathcal{B}} + \theta_{c\mathcal{B}}\right) + \dot{\theta}_{c\mathcal{B}}\dot{z}_{\mathcal{B}}\mathrm{c}\left(\theta_{\mathcal{B}} + \theta_{c\mathcal{B}}\right)\right) \\ & + \ell_{12} m_c\left(\dot{\theta}_{\mathcal{B}}\dot{z}_{\mathcal{B}}\mathrm{s}\theta_{\mathcal{B}} + \ell_2\left(\dot{\theta}_{\mathcal{B}}\dot{\theta}_{c\mathcal{B}}\mathrm{s}\theta_{c\mathcal{B}} + \dot{\theta}_{\mathcal{B}}^2\mathrm{s}\theta_{c\mathcal{B}}\right)\right) \\ & + \ell_2^2 m_c\left(\left(\dot{\theta}_{\mathcal{B}}^2 + \dot{\theta}_{c\mathcal{B}}^2\right) + 2\dot{\theta}_{\mathcal{B}}\dot{\theta}_{c\mathcal{B}}\right) \\ & + m_c\mathrm{g}\left(\ell_2\mathrm{s}\left(\theta_{\mathcal{B}} + \theta_{c\mathcal{B}}\right) + \ell_{12}\mathrm{c}\theta_{\mathcal{B}}\right) - z_{\mathcal{B}} m g \end{aligned} \tag{8}$$

by defining the generalized coordinates vector $\mathbf{q}_{\mathcal{L}}$ as

$$\mathbf{q}_{\mathcal{L}} = [\, x_{\mathcal{B}} \;\; z_{\mathcal{B}} \;\; \theta_{\mathcal{B}} \;\; \theta_{\mathcal{CB}} \,]^{\top} \tag{9}$$

The equation (eq. 8) is used for computing the multi-body motion equations, by direct application of the Lagrange formalism:

$$\begin{bmatrix} f_x \\ f_z \\ \tau_{\mathcal{B}} \\ \tau_{\mathcal{CB}} \end{bmatrix} = \frac{d}{dt}\left(\frac{\partial \mathcal{L}_{\mathcal{L}}}{\partial \dot{\mathrm{q}}_{\mathcal{L}}}\right) - \frac{\partial \mathcal{L}_{\mathcal{L}}}{\partial \mathrm{q}_{\mathcal{L}}} \tag{10}$$

Since we are interested in the evolution of the compounded system w.r.t. the inertial camera frame position, an additional conversion must be applied to the resulting equations. Hence, by defining the final generalized coordinates vector as

$$\mathbf{q} = [\, x_{\mathcal{C}} \;\; z_{\mathcal{C}} \;\; \theta_{\mathcal{B}} \;\; \theta_{\mathcal{C}} \,]^{\top} \tag{11}$$

and rewriting the motion equations by introducing

$$\theta_{\mathcal{C}} = \theta_{\mathcal{CB}} + \theta_{\mathcal{B}} \tag{12}$$

finally, undoing the previous translation between frames according to (Eq. 2), motion equations describing the evolution of the camera frame $[x_{\mathcal{C}} \;\; z_{\mathcal{C}} \;\; \theta_{\mathcal{C}}]^{\top}$ onboard the tPVTOL, are obtained. The total mass of the system is denoted as $m = m_{\mathcal{B}} + m_{\mathcal{C}}$, and $\mathrm{c}(\cdot)$ and $\mathrm{s}(\cdot)$ stands for $cos(\cdot)$ and $sin(\cdot)$, respectively.

2.4 Equations of motion

Through the Newton-Euler and Lagrange-Euler formulation, equations modeling the overall motion of the tPVTOL are derived. Set of equations (2) are used in (1) to get the absolute motion of the camera frame given by (3), considering translational and rotational motion of both systems as two interconnected dynamics (Castillo et al. (2005)). Hence, the translational subsystem evolution is described by the following equations:

$$\begin{cases} f_x = m\ddot{x}_{\mathcal{C}} + m_{\mathcal{B}}(\ell_{12}(\mathrm{c}\theta_{\mathcal{B}}\ddot{\theta}_{\mathcal{B}} - \mathrm{s}\theta_{\mathcal{B}}\dot{\theta}_{\mathcal{B}}^2) + \ell_2(\mathrm{s}\theta_{\mathcal{C}}\ddot{\theta}_{\mathcal{C}} + \mathrm{c}\theta_{\mathcal{C}}\dot{\theta}_{\mathcal{C}}^2)) \\ f_z = m(\ddot{z}_{\mathcal{C}}+\mathrm{g}) - m_{\mathcal{B}}\ell_{12}(\mathrm{s}\theta_{\mathcal{B}}\ddot{\theta}_{\mathcal{B}} + \mathrm{c}\theta_{\mathcal{B}}\dot{\theta}_{\mathcal{B}}^2) + m_{\mathcal{B}}\ell_2(\mathrm{c}\theta_{\mathcal{C}}\ddot{\theta}_{\mathcal{C}} - \mathrm{s}\theta_{\mathcal{C}}\dot{\theta}_{\mathcal{C}}^2) \end{cases} \tag{13}$$

and the rotational motion set of equations, which is not directly related with $\ddot{x}_{\mathcal{C}}$ and $\ddot{z}_{\mathcal{C}}$, as follows:

$$\begin{cases} \tau_{\mathcal{B}} = \tau_{\mathcal{CB}} + \mathrm{a}_1\ddot{\theta}_{\mathcal{B}} + \mathrm{a}_3(\mathrm{s}\theta_{\mathcal{CB}}\ddot{\theta}_{\mathcal{C}} + \mathrm{c}\theta_{\mathcal{CB}}\dot{\theta}_{\mathcal{C}}^2) \\ \tau_{\mathcal{CB}} = \mathrm{a}_2\ddot{\theta}_{\mathcal{C}} + \mathrm{a}_3(\mathrm{s}\theta_{\mathcal{CB}}\ddot{\theta}_{\mathcal{B}} + \mathrm{c}\theta_{\mathcal{CB}}\dot{\theta}_{\mathcal{B}}^2) - \mathrm{a}_4\mathrm{c}\theta_{\mathcal{CB}} \end{cases} \tag{14}$$

with:

$$\mathrm{a}_1 = I_{CM_{\mathcal{B}}} + \frac{m_{\mathcal{B}}m_{\mathcal{C}}}{m}\ell_{12}^2 \qquad \mathrm{a}_2 = I_c - \frac{m_{\mathcal{B}}m_{\mathcal{C}}}{m}\ell_2^2$$

$$\mathrm{a}_3 = \frac{m_{\mathcal{B}}m_{\mathcal{C}}}{m}\ell_{12}\ell_2 \qquad \mathrm{a}_4 = \tfrac{m_{\mathcal{C}}}{m}\ell_2$$

3. LINEAR CONTROL OF THE TPVTOL

In order to evaluate more sophisticated control structures, the study of linear control laws was previously proposed by authors in (Villagomez et al. (2014a)). A classical time-scale separation is considered between rotational (fast-dynamics inner loop) and translational motion (slow dynamics outer-loop). Both dynamics are partially decoupled and controlled by an attitude and position linear controllers.

3.1 Model asumptions and linearization

In hover mode the vehicle will operate in regions where $\theta_{\mathcal{B}} \backsimeq 0^o$. It will be used a linearized version of the nonlinear model obtained in (Eqs. 13-14), found by means of Taylor approximation in the vicinity of the nominal operating point. Considering the camera positioner angle around a fixed value ($\theta_{\mathcal{C}} \backsimeq 0^o$), the following equilibrium conditions are obtained:

$$\begin{array}{llll} \theta_{\mathcal{B}}^{eq} = 0 & \tau_{\mathcal{B}}^{eq} = \tau_{\mathcal{CB}}^{eq} + m_{\mathcal{C}}\mathrm{g}\ell_{12}\mathrm{s}\theta_{\mathcal{B}}^{eq} = & \tau_{\mathcal{CB}}^{eq} \\ \theta_{\mathcal{C}}^{eq} = 0 & \tau_{\mathcal{CB}}^{eq} = -m_{\mathcal{C}}\mathrm{g}\ell_2\mathrm{c}\theta_{\mathcal{C}}^{eq} & = -m_{\mathcal{C}}\mathrm{g}\ell_2 \\ f^{eq} = \dfrac{m\mathrm{g}}{\mathrm{c}\theta_{\mathcal{B}}^{eq}} & & \end{array} \tag{15}$$

given by the small value increment (small angle assumption) of the generalized coordinates:

$$\begin{array}{lll} \tau_{\mathcal{B}}(t) = \tau_{\mathcal{B}}^{eq} + \tau_{\mathcal{B}}^{\delta}(t) & x_{\mathcal{C}}(t) = x_{\mathcal{C}}^{eq} + x_{\mathcal{C}}^{\delta}(t) & \theta_{\mathcal{B}}(t) = \theta_{\mathcal{B}}^{eq} + \theta_{\mathcal{B}}^{\delta}(t) \\ \tau_{\mathcal{CB}}(t) = \tau_{\mathcal{CB}}^{eq} + \tau_{\mathcal{CB}}^{\delta}(t) & z_{\mathcal{C}}(t) = z_{\mathcal{C}}^{eq} + z_{\mathcal{C}}^{\delta}(t) & \theta_{\mathcal{C}}(t) = \theta_{\mathcal{C}}^{eq} + \theta_{\mathcal{C}}^{\delta}(t) \\ f(t) = f^{eq} + f^{\delta}(t) & & \end{array} \tag{16}$$

whatever $x_{\mathcal{C}}^{eq}$ and $z_{\mathcal{C}}^{eq}$ coordinates. This assumption leads to the following time-invariant linearized representation of the system, i.e. the translational:

$$\ddot{x_{\mathcal{C}}^{\delta}}(t) = \tfrac{f^{eq}}{m}\theta_{\mathcal{B}}^{\delta}(t) - \tfrac{m_{\mathcal{B}}\ell_{12}}{m}\ddot{\theta}_{\mathcal{B}}^{\delta}(t) \tag{17}$$

$$\ddot{z_{\mathcal{C}}^{\delta}}(t) = \tfrac{f^{\delta}(t)}{m} - \tfrac{m_{\mathcal{B}}\ell_2}{m}\ddot{\theta}_{\mathcal{C}}^{\delta}(t) \tag{18}$$

and the rotational subsystem:

$$\tau_{\mathcal{B}}^{\delta}(t) - \tau_{\mathcal{CB}}^{\delta}(t) = \mathrm{a}_1\ddot{\theta}_{\mathcal{B}}^{\delta}(t) + \mathrm{a}_3\mathrm{s}\theta_{\mathcal{CB}}^{eq}\ddot{\theta}_{\mathcal{C}}^{\delta}(t) \tag{19}$$

$$\begin{aligned} \tau_{\mathcal{CB}}^{\delta}(t) = {} & \mathrm{a}_2\ddot{\theta}_{\mathcal{C}}^{\delta}(t) + \mathrm{a}_3\mathrm{s}\theta_{\mathcal{CB}}^{eq}\ddot{\theta}_{\mathcal{B}}^{\delta}(t) \\ & - \mathrm{a}_4\mathrm{c}\theta_{\mathcal{CB}}^{eq}f^{\delta}(t) + m_{\mathcal{C}}\mathrm{g}\ell_2\mathrm{s}\theta_{\mathcal{CB}}^{eq}\theta_{\mathcal{CB}}^{\delta}(t) \end{aligned} \tag{20}$$

Based on equations (16-20) in the time domain, the application of Laplace transformation yield the following transfer functions, which are considered for the control tasks:

$$\mathrm{x}_{\mathcal{C}}(\mathrm{s}) = \tfrac{1}{m\mathrm{s}^2}(f^{eq} - m_{\mathcal{B}}\ell_{12}\mathrm{s}^2)\theta_{\mathcal{B}}(\mathrm{s}) \tag{21}$$

$$\mathrm{z}_{\mathcal{C}}(\mathrm{s}) = \tfrac{1}{m\mathrm{s}^2}f(\mathrm{s}) - \tfrac{m_{\mathcal{B}}}{m}\ell_2\theta_{\mathcal{C}}(\mathrm{s}) \tag{22}$$

$$\theta_{\mathcal{B}}(\mathrm{s}) = \tfrac{1}{\mathrm{a}_1\mathrm{s}^2}(\tau_{\mathcal{B}}(\mathrm{s}) - \tau_{\mathcal{CB}}(\mathrm{s})) \tag{23}$$

$$\theta_{\mathcal{C}}(\mathrm{s}) = \tfrac{1}{\mathrm{a}_2\mathrm{s}^2}(\tau_{\mathcal{CB}}(\mathrm{s}) + \mathrm{a}_4 f(\mathrm{s})) \tag{24}$$

where, e.g., $\mathrm{x}_{\mathcal{C}}(\mathrm{s}) = \mathscr{L}[x_{\mathcal{C}}^{\delta}(t)]$. The root locus analysis method was used to synthesize and tuning the linear control laws.

3.2 Rotational subsystem controller

From equations (23-24) it is possible to synthesize a linear controller for stabilizing the rotational subsystem, whose evolution depends directly on input moments $\tau_{\mathcal{B}}$ and $\tau_{\mathcal{CB}}$. To deal with sustained disturbances motivated by gravity effects and changing thrust input, a feed-forward term is supplied to the controller output for the camera's *tilt* angle (Eq.26)(Fig. 2). The control design process must provide stability and quick system response to the inner-loop (rotational subsystem) to guarantee the effectiveness of the outer-loop control (translational

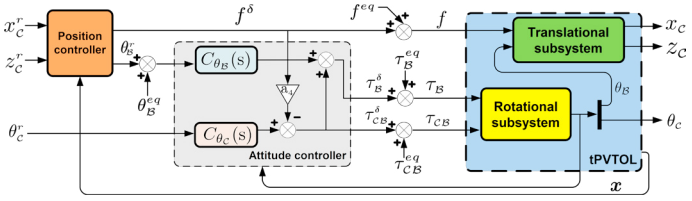

Figure 2. Depiction of the proposed linear control scheme: the translational motion of the tPVTOL is controlled thought the heading's angle ($\theta_{\mathcal{B}}$) and input thrust (f). Camera's *tilt*-angular position is pre-compensated to reject thrust input changing effects.

motion). Controller expressions for the stabilization of the rotational subsystem: MAV's pitch angle ($\theta_{\mathcal{B}}$)

$$C_{\theta_{\mathcal{B}}}(\mathrm{s}) = \frac{34.51\mathrm{s} + 690.2}{0.001667\mathrm{s} + 1} \tag{25}$$

and camera's tilt position:

$$C_{\theta_{\mathcal{C}}}(\mathrm{s}) = \frac{20.23\mathrm{s} + 404.5}{0.001667\mathrm{s} + 1} \tag{26}$$

are provided.

3.3 Translational subsystem controller

Translational $x_{\mathcal{C}}$ component control expression (Eq. 27) is quite constrained for the evidence of a non-minimum phase zero in (Eq. 21), being underactuated by the $\theta_{\mathcal{B}}$ angle and input thrust on its equilibrium value (Eq. 15). Nevertheless, the height of the camera frame can be directly controlled (Eq. 28) since there is direct action over the variables which $z_{\mathcal{C}}$ has dependence on. Output signals of the translational subsystem controller, based on PD controllers, will be used as input references in the rotational subsystem.

$$C_{x_{\mathcal{C}}}(\mathrm{s}) = \frac{0.1515\mathrm{s} + 0.0752}{0.002536\mathrm{s}^2 + 0.1007\mathrm{s} + 1} \tag{27}$$

$$C_{z_{\mathcal{C}}}(\mathrm{s}) = \frac{21.68\mathrm{s} + 86.72}{0.008333\mathrm{s} + 1} \tag{28}$$

4. NON-LINEAR CONTROL OF THE TPVTOL

In this section we present the nonlinear control strategies, which are based on a hierarchical scheme considering the time-scale separation between rotational and translational dynamics. We propose to use standard Backstepping and Sliding-mode approaches, to control the internal loop (rotational) and outer-loop dynamics. These control techniques were previously considered and tested on the particular case where references are provided in the MAV frame (Villagomez et al. (2014b)).

4.1 Space state representation

The model (Eqs. 13-14) shall be rewritten in a state-space form $\dot{\boldsymbol{x}} = f(\boldsymbol{x}, \mathbf{u})$ by introducing $\boldsymbol{x} = [x_1 ... x_8]^\top \in \mathbb{R}^8$ as the state vector of the system:

$$\begin{array}{l|l} x_1 = \theta_{\mathcal{B}} & x_5 = x_{\mathcal{C}} \\ x_2 = \dot{\theta}_{\mathcal{B}} & x_6 = \dot{x}_{\mathcal{C}} \\ x_3 = \theta_{\mathcal{C}} & x_7 = z_{\mathcal{C}} \\ x_4 = \dot{\theta}_{\mathcal{C}} & x_8 = \dot{z}_{\mathcal{C}} \end{array} \tag{29}$$

It is possible to obtain a reduced model, discarding effects provided by lateral accelerations or centripetal forces in near-hovering flights conditions. These assumptions yield a simplification of the space-state system representation, considered for the control law design, which is stated through the following vector:

$$\dot{\boldsymbol{x}} = \begin{bmatrix} x_2 \\ \frac{1}{b_1}(\mathrm{u}_3 - \mathrm{c}\,(x_1 - x_3)\left(\mathrm{a}_3\left(x_2^2 + x_4^2\right) - \mathrm{a}_4\right)) \\ x_4 \\ \frac{1}{\mathrm{a}_2}(\mathrm{u}_4 + \mathrm{c}\,(x_1 - x_3)\,\left(\mathrm{a}_4 - \mathrm{a}_3 x_2^2\right)) \\ x_6 \\ \frac{1}{m}(\mathrm{u}_1 + \mathrm{a}_5 \mathrm{s} x_1 x_2^2 - \mathrm{a}_6 \mathrm{c} x_3 x_4^2) \\ x_8 \\ \frac{1}{m}(\mathrm{u}_2 - \mathrm{g}m + m_{\mathcal{B}}\left(\ell_{12}\mathrm{c}x_1 x_2^2 + \ell_2 \mathrm{s} x_3 x_4^2\right)) \end{bmatrix} \tag{30}$$

where:

$$\mathrm{a}_5 = m_{\mathcal{B}}\ell_{12} \qquad \mathrm{a}_6 = m_{\mathcal{B}}\ell_2 \qquad \mathrm{b}_1 = \mathrm{a}_1\mathrm{a}_2 - \mathrm{a}_3^2\,\mathrm{s}\,(\mathrm{x}_1 - \mathrm{x}_3)^2$$

and the control input vector stated as:

$$\mathbf{u} = \begin{bmatrix} \mathrm{u}_1 \\ \mathrm{u}_2 \\ \mathrm{u}_3 \\ \mathrm{u}_4 \end{bmatrix} = \begin{bmatrix} f_x \\ f_z \\ \tau_{\mathcal{B}} \\ \tau_{\mathcal{CB}} \end{bmatrix} = \begin{bmatrix} f \cdot \sin(\theta_{\mathcal{B}}) \\ f \cdot \cos(\theta_{\mathcal{B}}) \\ (f_2 - f_1)\ell \\ \tau_{\mathcal{CB}} \end{bmatrix} \tag{31}$$

In order to track a desired trajectory in the space, the computation of virtual control inputs u_1 and u_2 provides the required pitch angle and total input thrust to command the attitude controller and the platform rotors, respectively. Hence, the design of nonlinear controllers is based on a cascade control scheme where the attitude controller provides control inputs u_3 and u_4 to the tPVTOL in combination with total input thrust f provided by the position controller (Fig. 3).

4.2 Backstepping controller design

Using the Backstepping approach, based on (Bouabdallah and Siegwart (2005)), it is possible to synthesize the virtual control law forcing the system to follow the desired trajectory, since it is possible to design a method to backstep the control input given the obtained model (Eq. 30).

Attitude controller For the first step, the tracking error can be considered as:

$$z_1 \triangleq x_1^r - x_1 \tag{32}$$

where, e.g., x_1^r defines the desired heading of the tPVTOL (Eq. 29). By considering the Lyapunov theorem of stability, we define a Lyapunov function on z_1 positive definite

$$V(z_1) = \tfrac{1}{2} z_1^2 \tag{33}$$

and its time derivative as:

$$\dot{V}(z_1) = z_1(\dot{x}_1^r - x_2) \tag{34}$$

The stabilization of z_1 is obtained introducing a virtual control input x_2 as

$$x_2 = \dot{x}_1^r + \alpha_1 z_1 \tag{35}$$

with $\alpha_1 > 0$. The equation (34) is rewritten as:

$$\dot{V}(z_1) = -\alpha_1 z_1^2 \tag{36}$$

by changing variables:

$$z_2 = x_2 - \dot{x}_1^r - \alpha_1 z_1 \tag{37}$$

For the second step, the following augmented Lyapunov function is considered:

$$V(z_1, z_2) = \tfrac{1}{2}(z_1^2 + z_2^2) \tag{38}$$

The corresponding time derivative of (38) is:

$$\dot{V}(z_1,z_2) = z_2(\tfrac{1}{b_1}(u_3 - c\,(x_1 - x_3)\,(a_3\,(x_2^2 + x_4^2) - a_4))) - z_2(\ddot{x}_1^r - \alpha_1(z_2 + \alpha_1 z_1)) - z_1(z_2 - \alpha_1 z_1) \quad (39)$$

Finally, considering zero the reference in the desired acceleration ($\ddot{x}_1^r = 0$), the control output u_3 is then extracted, satisfying $\dot{V}(z_1,z_2) < 0$:

$$u_3 = (z_1 - \alpha_1(z_2 + \alpha_1 z_1) - \alpha_2 z_2)\,b_1 + (c(x_1 - x_3)(a_3 x_2^2 + a_3 x_4^2 - a_4)) \quad (40)$$

Term $\alpha_2 z_2$ is added in order to stabilize z_1. A similar procedure is performed to compute the input control u_4:

$$u_4 = (z_3 - \alpha_3(z_4 + \alpha_3 z_3) - \alpha_4 z_4)\,a_2 - (c(x_1 - x_3)(-a_3 x_2^2 + a_4)) \quad (41)$$

with:

$$z_3 = x_3^r - x_3 \qquad z_4 = x_4 - \dot{x}_3^r - \alpha_3 z_3 \quad (42)$$

Position controller The procedure followed to compute control signals u_1 and u_2 is similar to the previous section.

$$u_1 = (z_5 - \alpha_5(z_6 + \alpha_5 z_5) - \alpha_6 z_6)\,m - (a_5 s x_1 x_2^2) + (a_6 x_4^2 c x_3) \quad (43)$$

$$u_2 = (z_7 - \alpha_7(z_8 + \alpha_7 z_7) - \alpha_8 z_8)\,m - \ell_{12} m_{\mathcal{B}} c x_1 x_2^2 - \ell_2 m_{\mathcal{B}} s x_3 x_4^2 + gm \quad (44)$$

with:

$$z_5 = x_5^r - x_5 \qquad z_6 = x_6 - \dot{x}_5^r - \alpha_5 z_5$$
$$z_7 = x_7^r - x_7 \qquad z_8 = x_8 - \dot{x}_7^r - \alpha_7 z_7 \quad (45)$$

Similarly, terms $\alpha_6 z_6$ and $\alpha_8 z_8$ with $(\alpha_6, \alpha_8) > 0$ are added to stabilize virtual control laws z_5 and z_7, respectively.

4.3 Sliding-mode controller design

The first step concerning the design of a Sliding-mode based control law is similar to the one used for the backstepping approach, using the state-space system defined in (Eq. 30).

Attitude controller For the rotational subsystem, instead of using a second virtual control variable as z_2, the surface s_2 is used to be consistent with the Sliding-mode law definition:

$$s_2 \triangleq x_2 - \dot{x}_1^r - \alpha_1 z_1 \quad (46)$$

For the second step, we consider the augmented Lyapunov function:

$$V(z_1, s_2) = \tfrac{1}{2}(z_1^2 + s_2^2) \quad (47)$$

The chosen law for the attractive surface is the time derivative of (46) satisfying ($s\dot{s} < 0$):

$$\dot{s}_2 = -k_1\mu(s_2) - k_2 s_2 = \dot{x}_2 - \ddot{x}_1^r - \alpha_1 \dot{z}_1 = \tfrac{1}{b_1}(u_3 - c(x_1 - x_3)(a_3 x_2^2 + a_3 x_4^2 - a_4)) - \ddot{x}_1^r + \alpha_1(s_2 + \alpha_1 z_1) \quad (48)$$

The control signal u_3 is then extracted:

$$u_3 = (-\alpha_1^2 z_1 - k_1\mu(s_2) - k_2 s_2)\,b_1 + c(x_1 - x_3)(a_3 x_2^2 + a_3 x_4^2 - a_5) \quad (49)$$

And the same step is followed in order to get u_4:

$$u_4 = (-\alpha_2^2 z_3 - k_3\mu(s_4) - k_4 s_4)\,a_2 - c(x_1 - x_3)(-a_3 x_2^2 + a_4) \quad (50)$$

with:

$$z_3 = x_3^r - x_3 \qquad s_3 = x_4 - \dot{x}_3^r - \alpha_2 z_3 \quad (51)$$

Param.	g	$m_{\mathcal{C}}$	$m_{\mathcal{B}}$	$I_{CM_{\mathcal{B}}}$	$I_{\mathcal{C}}$	ℓ_1	ℓ_2	ℓ_{11}
Value	9.81	0.4	0.955	0.43	0.25	0.10	0.10	0.03
Unit	$\frac{m}{s^2}$	kg		$kg \cdot m^2$		m		

Table 1. System model parameter values

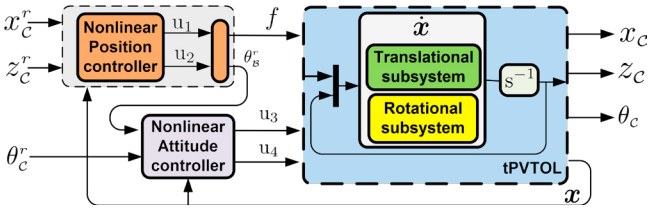

Figure 3. Overview of the proposed control scheme and the decomposition of coupled subsystems.

Position controller Following a similar procedure, control signals u_1 and u_2 are then computed and extracted:

$$u_1 = (-\alpha_3^2 z_5 - k_5\mu(s_6) - k_6 s_6)\,a_2 - (a_5 s x_1 x_2^2 - a_6 c x_3 x_4^2) \quad (52)$$

$$u_2 = (-\alpha_4^2 z_7 - k_7\mu(s_8) - k_8 s_8)\,a_2 - (m_{\mathcal{B}}(\ell_{12} c x_1 x_2^2 + \ell_2 s x_3 x_4^2) - gm) \quad (53)$$

with:

$$z_5 = x_5^r - x_5 \qquad s_4 = x_6 - \dot{x}_5^r - \alpha_3 z_5$$
$$z_7 = x_7^r - x_7 \qquad s_5 = x_8 - \dot{x}_7^r - \alpha_4 z_7 \quad (54)$$

5. CONTROL STRATEGIES PERFORMANCE

The main aim is to control the camera frame position ($[x_c \;\; z_c]^\top = [x_5 \;\; x_7]^\top$) and its *tilt* angle ($\theta_c = x_3$). The proposed control strategies will be tested by simulation, considering system parameter values collected in table (Tab. 1), close to real aerial platforms. The evaluation of the linear control strategies is performed following the control scheme depicted in (Fig. 2). Corresponding preliminary results obtained by authors in (Villagomez et al. (2014a)) are to be assessed with the full space-state system representation (13-14) and the nonlinear controllers proposed in (Villagomez et al. (2014b)) following the control scheme depicted in (Fig. 3). Neither disturbance nor uncertainty terms are considered for the simulation process. Propellers forces and control inputs for the translational subsystem f_x and f_z would be limited, with a value not exceeding $f_{max} = 2mg = 26.58$ N. Similarly, the maximum torque provided by the camera positioner rotational joint not exceeds $|\tau_{c\mathcal{B}}| \leq 4m_c g\ell_2 = 1.56$ N·m. The heading reference angle computed by the translational controller will be bounded: $|\theta_{\mathcal{B}}^r| < 0.34\,rad$. Function $\mu(x)$ is proposed as an alternative to the non-continuous $sign(x)$ function (Villagomez et al. (2014b)).

Nonlinear controller parameters of the Backstepping (Tab. 2) and Sliding-mode (Tab. 3) techniques were simultaneously adjusted by observing the behaviour of the system in closed loop. Initial conditions are $[x_c \;\; z_c]_0^\top = [0 \;\; 0]^\top(m)$ for the translational subsystem, and $[\theta_{\mathcal{B}} \;\; \theta_c]_0^\top = [0 \;\; 0]^\top(rad)$ for the rotational case. The goal for the control task was to achieve the desired position $[x_{\mathcal{C}}^r \;\; z_{\mathcal{C}}^r]^\top$ fully stabilized in a desired orientation ($\theta_{\mathcal{C}}^r$).

5.1 Attitude controller

Rotational subsystem evolution in closed loop (Fig. 4) with input changing references is satisfactory in terms of system

Parameter	α_1	α_2	α_3	α_4	α_5	α_6	α_7	α_8
Value	30	15	20	10	20	15	8.5	5

Table 2. Proposed parameter values for the Backstepping controller.

Control input signal

u_1		u_2		u_3		u_4	
α_3	5	α_4	3	α_1	4	α_2	5
k_5	5	k_7	10	k_1	3.5	k_3	4
k_6	7	k_8	10	k_2	3.5	k_4	4

Table 3. Proposed parameter values for the Sliding-mode controller.

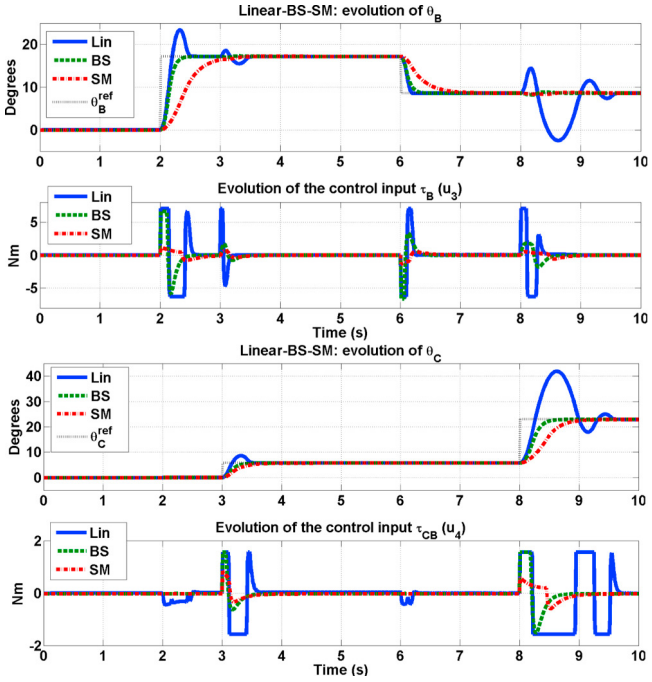

Figure 4. Simulation: evolution of the θ_B and θ_c component in closed loop with linear and nonlinear techniques.

time response and zero error in stationary. Numerical results obtained show that the proposed controllers are able to stabilize rotational subsystem.

5.2 Position controller

The application of the nonlinear control techniques leads the system to avoid disturbances motivated by the coupling dynamics with more conservative control commands than the linear case. Although the trajectory-tracking objective is fulfilled, the system behaviour in closed loop with nonlinear schemes is more satisfactory than those obtained previously by the authors in (Villagomez et al. (2014a)), as depicted in figure (Fig. 5).

6. FINAL REMARKS AND PERSPECTIVES

This paper addressed the planar modeling and control of a multi-body aerial platform consisting of a MAV and a camera positioner. The aim is to use the two additional degrees of freedom provided by a camera positioner in combination with an under-actuated quad-rotor aircraft to get a fully actuated system, allowing free arbitrary movement of the camera in the space. The application of

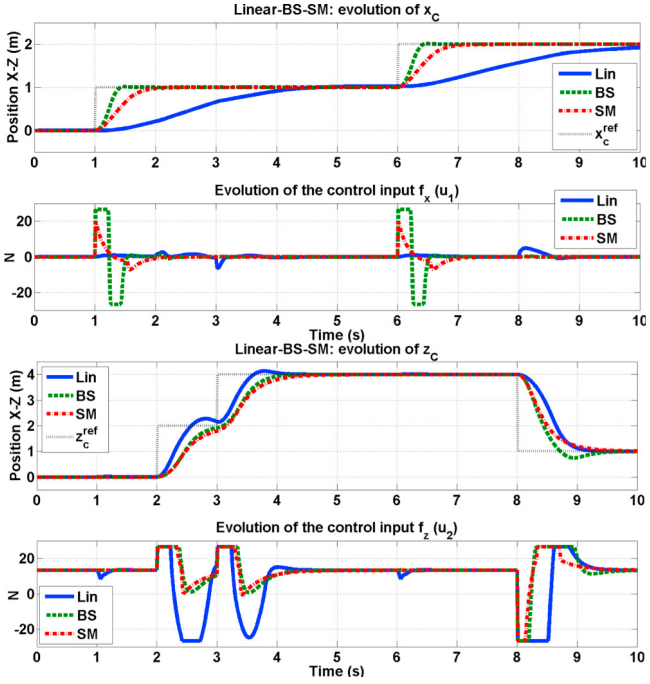

Figure 5. Simulation: evolution of the translational subsystem x_c and z_c component in closed loop with the proposed controllers

the Backstepping approach provides, in general, satisfactory results in stabilizing the full system dynamics. First tuning of the Sliding-mode controller provides good results in stabilizing inner and outer-loop, but it is highly sensitive to the system model parameters. Upcoming working lines will comprise deeper study of parameter assignment and the effects on the stabilization of the tPVTOL and the modeling of the multi-body aerial platform proposed in this work to the space.

REFERENCES

Altug, E., Ostrowski, J., and Mahony, R. (2002). Control of a quadrotor helicopter using visual feedback. *Proceedings ICRA. IEEE International Conference on Robotics and Automation*, 1, 72–77.

Bouabdallah, S. and Siegwart, R. (2005). Backstepping and sliding-mode techniques applied to an indoor micro quadrotor. *Proceedings ICRA. IEEE International Conference on Robotics and Automation*.

Castillo, P., Lozano, R., and Dzul, A. (2005). *Modelling and Control of Mini-Flying Machines*. Springer.

Kim, S., Choi, S., and Kim, H. (2013). Aerial manipulation using a quadrotor with a two dof robotic arm. In *Intelligent Robots and Systems (IROS), 2013 IEEE/RSJ International Conference on*, 4990–4995. doi:10.1109/IROS.2013.6697077.

Kondak, K., Huber, F., Schwarzbach, M., Laiacker, M., Sommer, D., Bejar, M., and Ollero, A. (2014). Aerial manipulation robot composed of an autonomous helicopter and a 7 degrees of freedom industrial manipulator. In *Robotics and Automation (ICRA), 2014 IEEE International Conference on*, 2107–2112. doi:10.1109/ICRA.2014.6907148.

Neff, A., Lee, D., Chitrakaran, V., Dawson, D., and Burg, T. (2007). Velocity control for a quad-rotor UAV fly-by-camera interface. *SoutheastCon. Proceedings IEEE*, 273–278.

Orsag, M., Korpela, C., Pekala, M., and Oh, P. (2013). Stability control in aerial manipulation. In *American Control Conference (ACC), 2013*, 5581–5586. doi:10.1109/ACC.2013.6580711.

Villagomez, J., Vargas, M., Ortega, M., and Rubio, F. (2014a). Planar modeling of an actuated camera onboard a MAV. *In Proceedings of the 11th Portuguese Conference on Automatic Control, CONTROLO*.

Villagomez, J., Vargas, M., and Rubio, F. (2014b). Backstepping and sliding-mode techniques applied to an underactuated camera onboard a rotorcraft mav. In *3rd Workshop on Visual Control of Mobile Robots, Vicomor.*, 1–7.